The 25th IEEE International Conference on Intelligent Transportation Systems (ITSC 2022)

CORM: Constrained Optimal Reconfiguration Matrix for Safe On-Ramp Cooperative Merging of Automated Vehicles

Lyes Saidi [1], Lounis Adouane [1] and Reine Talj [1]

[1] Heudiasyc laboratory, University of Technology of Compiègne, France

Macau, China 8th -12th of October 2022

Context & Goals

Context:

On-ramp merging on highway performed by Autonomous Vehicles (AVs)

On-ramp merging on highway performed by Cooperative and Automated Vehicles (CAVs)

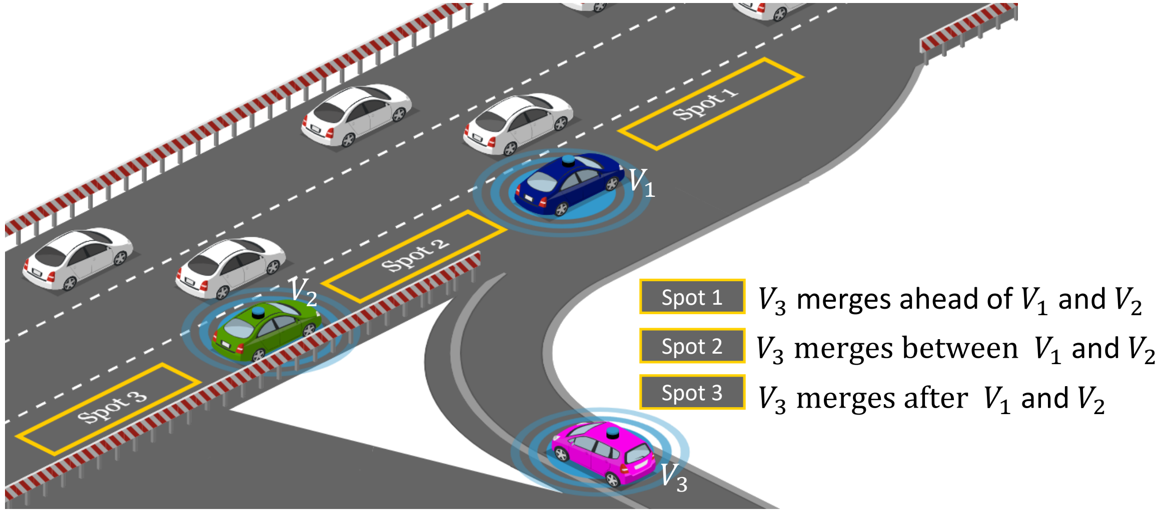

Fig 1. On-ramp merging on highway performed by AVs

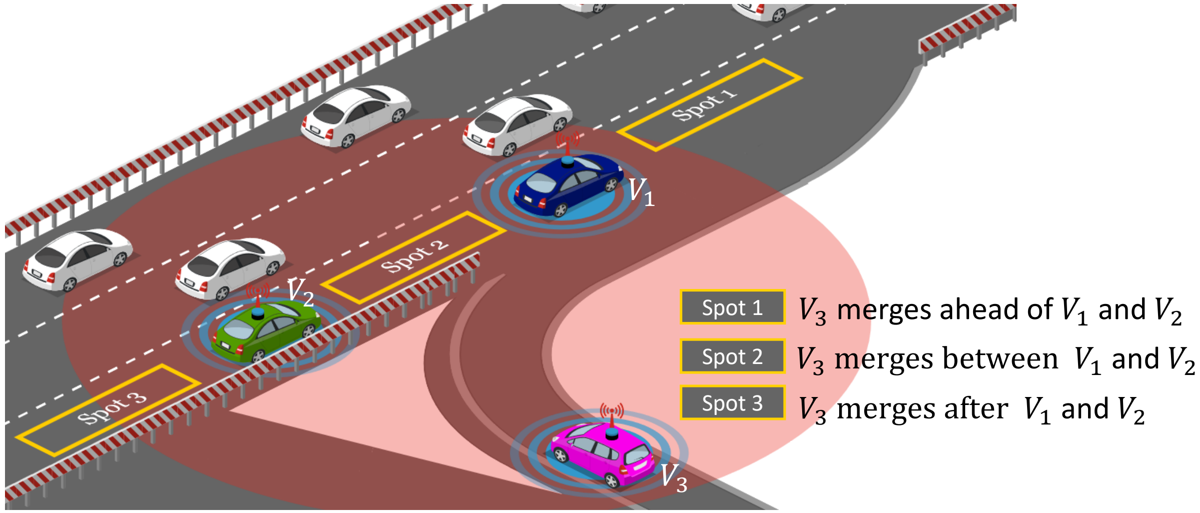

Fig 2. On-ramp merging on highway performed by CAVs

- **Ego-centered** resulting merging maneuver,
- Lake of **anticipation** and **synchronization**,
- Not **efficient** in terms of **energy consumption**.

- **Cooperative** on-ramp merging maneuver,
- **Anticipation** is improved using surrounding CAVs information shared using communication,
- Synchronization permits to improve the energy **efficiency.**

Goals:

- Adapt the **inter-target distance matrix** proposed in [1] for open world to on-road constrained environment,
- Ensure **safe and smooth on-ramp merging on highway maneuver** for CAVs.

[1] J. Vilca, L. Adouane and M. Youcef, Stable and Flexible Multi-Vehicle Navigation Based on Dynamic Inter-Target Distance Matrix, IEEE Transactions on Intelligent Transportation Systems, vol 20, pp. 1416- 1431, 2019.

Multi-level architecture for decision making, global and local planning

Decision making:

- Set the *passing order of the CAVs in the merging zone*, using between the CAVs.

Global planning level:

- Define the *global reference path* of each CAV part of the formation according to the road topology.

The details on the parts 1 and 2 are out of the scope of this paper.

Local planning level:

- Using the *passing order* and the *global reference path* of the CAVs, this level is in charge of *trajectory planning*.

Its goals:

- Ensure the respect of the *passing order*,
- Track the *global reference path*,
- Take advantage from the CAVs interactions to perform *safe and smooth merging maneuver*.

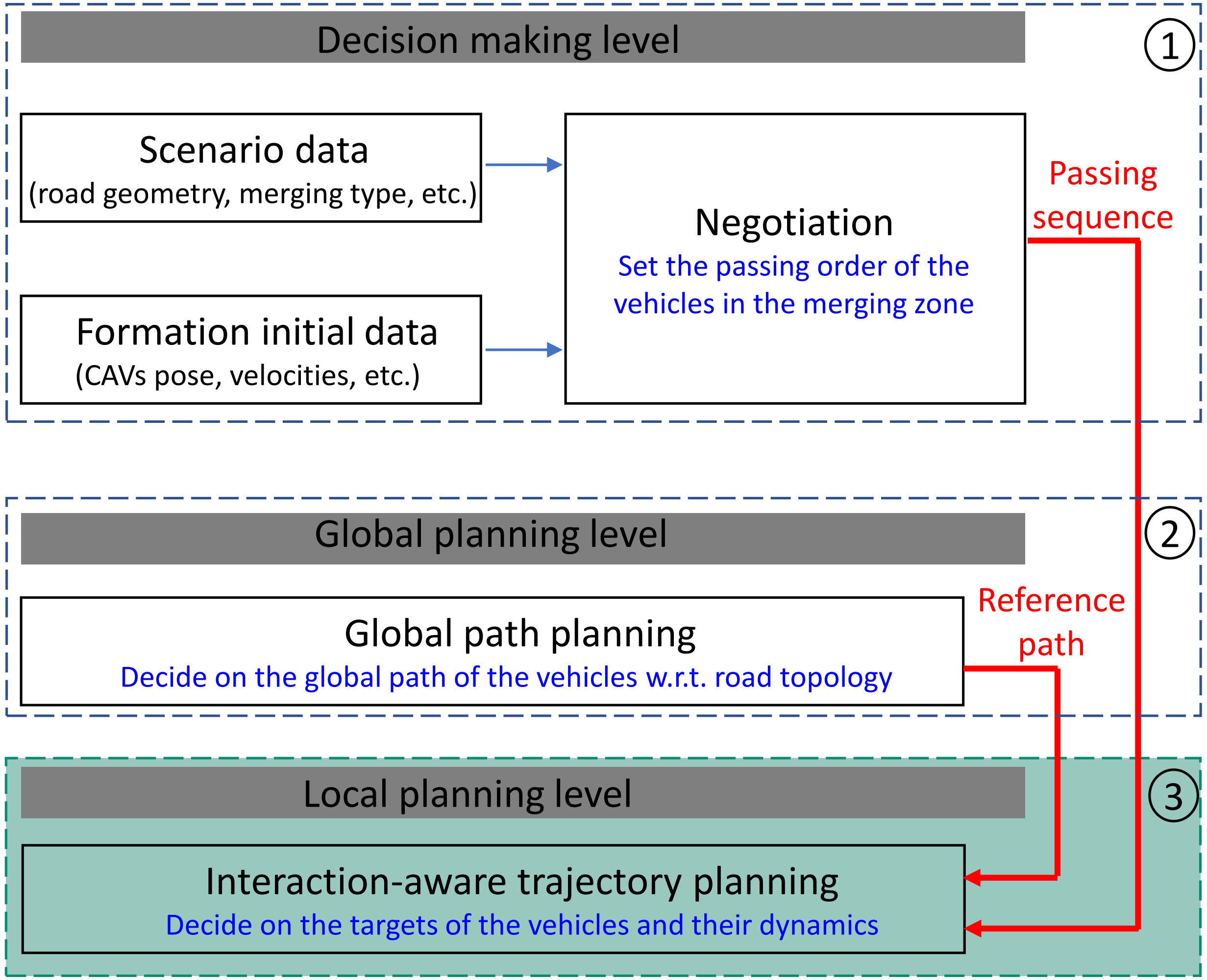

Fig 3. Overall architecture on the different levels of decision and global/local path and trajectory planning

Plan

- Problem statement
- Constrained optimal reconfiguration matrix
- Safe and feasible on-ramp merging maneuver
- Simulation results
- Conclusion and perspectives

Problem statement

Virtual structure formation modeling

- The **communication range C_R** is used to define the CAVs part of the formation.
- $N \in \mathbb{N}$ is the number of the CAVs under $\mathbf{C_R}$
- i is the *indices* of the considered CAV.
- $\mathcal{N} = \{1, \ldots, N\}$ the *set representing all the CAVs indices*.
- The initial pose $[X, Y, \theta]^T$ and velocity $\mathcal{V}$ of each CAV are known.
- A **Frenet reference** frame based on V_R is used to compute the coordinates of the CAVs part of the formation.

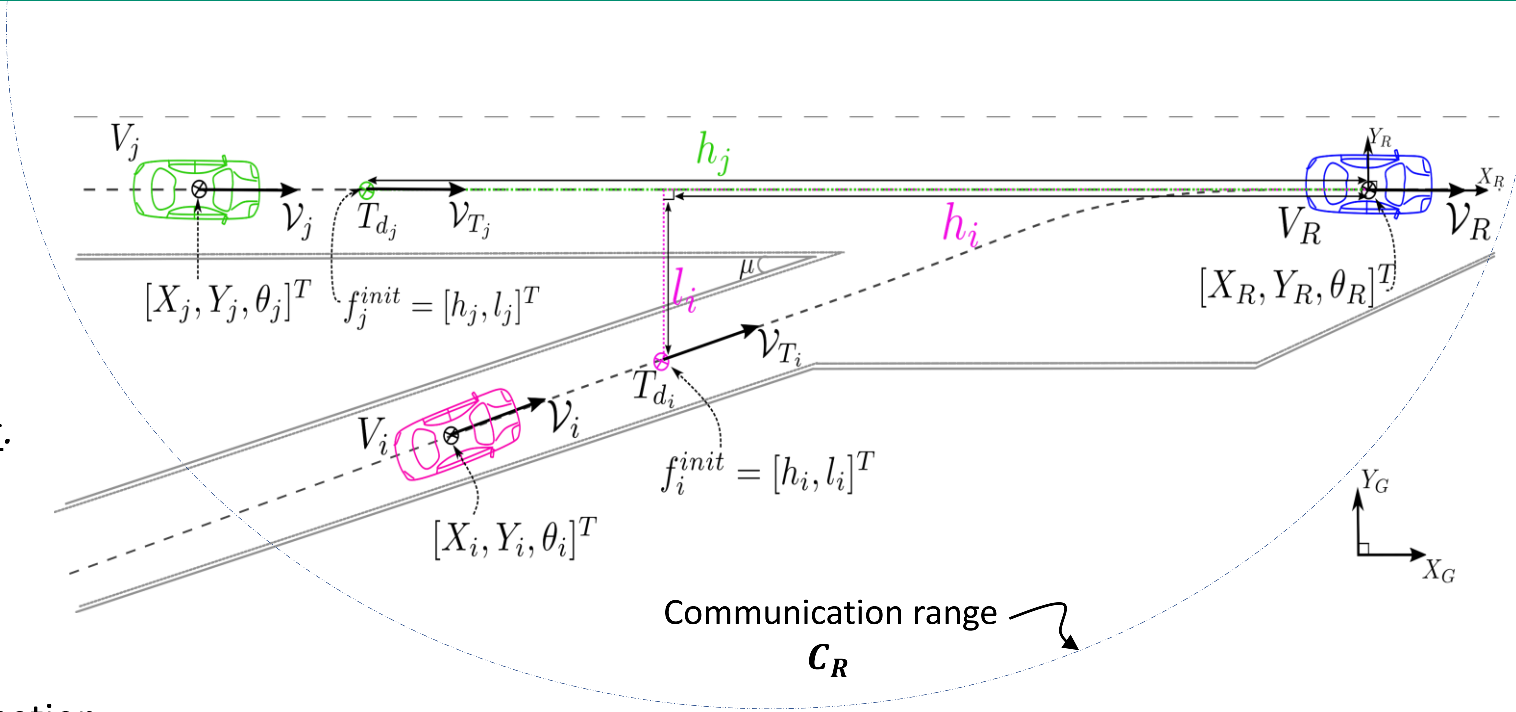

Fig 4. Virtual structure formation modeling framework

- $\boldsymbol{h}$ and $\boldsymbol{l}$ are respectively, *the longitudinal and lateral coordinates* w.r.t. V_R's pose.
- The shape of the **virtual structure** is defined by *the virtual targets* $\boldsymbol{T_d}$.
- The transformation from the mobile reference to the global reference is obtained with:

$$\begin{bmatrix} x_{T\,i} \\ y_{T\,i} \end{bmatrix} = \begin{bmatrix} x_R(h_i) \\ y_R(l_i) \end{bmatrix} + \begin{bmatrix} -l_i \sin(\theta_R(h_i)) \\ l_i \cos(\theta_R(h_i)) \end{bmatrix} \qquad (1)$$

Virtual structure formation modeling

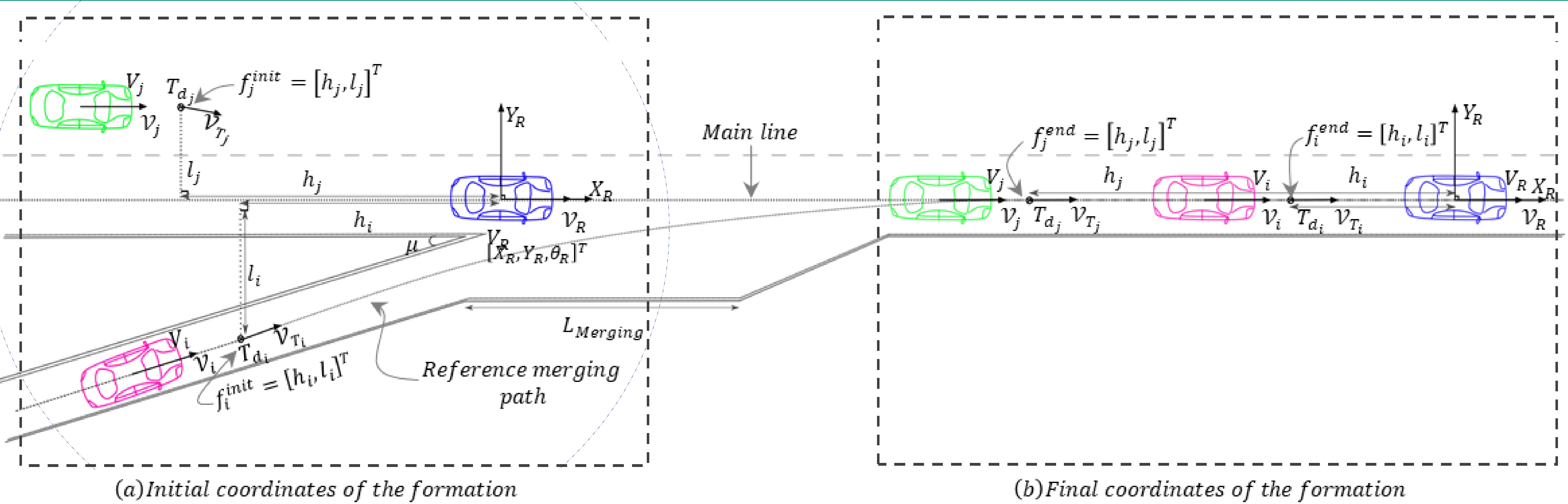

Fig 5. The virtual structure approach used to model the formation and its reconfiguration to perform the merging maneuver. (a) The initial shape of the formation and its coordinates. (b) The final shape of the formation after the merging maneuver and its desired coordinates.

The initial coordinates of the formation

$$F^{init} = \begin{bmatrix} h_i & h_j & \cdots & h_N \\ l_i & l_j & \cdots & l_N \end{bmatrix}$$

The intermediary coordinates of the formation

$$\boldsymbol{F(t)} = \begin{bmatrix} \boldsymbol{h_i} & \boldsymbol{h_j} & \cdots & \boldsymbol{h_N} \\ \boldsymbol{l_i} & \boldsymbol{l_j} & \cdots & \boldsymbol{l_N} \end{bmatrix}$$

The final coordinates of the formation

$$F^{end} = \begin{bmatrix} h_i & h_j & \cdots & h_N \\ l_i & l_j & \cdots & l_N \end{bmatrix}$$

With $N \epsilon \mathbb{N}$ | $\mathcal{N} = \{1, \cdots, N\}$ | $i, j \in \mathcal{N}$ where N is the number of the CAVs part of the formation.

Inter-target distance matrix formalization

The **convergence error e_{f_i}** between *the initial* and *the final coordinate* of the CAV_i part of the formation:

$$e_{f_i} = f_i^{end} - f_i(t) \qquad (2)$$

The **global convergence error e_F** for a formation composed of N CAVs can be written as:

$$e_F = F^{end} - F(t) \qquad (3)$$

With $F^{end} = \begin{bmatrix} h_i & h_j & \cdots & h_N \\ l_i & l_j & \cdots & l_N \end{bmatrix}$ And $F(t) = \begin{bmatrix} h_i & h_j & \cdots & h_N \\ l_i & l_j & \cdots & l_N \end{bmatrix}$

The **convergence error rate** is known as: $\dot{e}_F = g\left(e_{f_i}, e_{f_j}, \ldots, e_{f_N}\right) \qquad (4)$

A *first order dynamic* is used to characterize the evolution of the convergence error *while ensuring the in-between distance within the formation members*:

$$\dot{e}_F = Ae_F \qquad (5)$$

With

$$A = \begin{bmatrix} a_1 & a_{12} & \ldots & a_{1N} \\ -a_{12} & a_2 & \ldots & a_{2N} \\ \vdots & \vdots & \ddots & \vdots \\ -a_{1N} & -a_{2N} & \cdots & a_N \end{bmatrix} \qquad (6)$$

$a_i \mid \forall i \in \mathcal{N}$ control **the convergence rate of the error**

$a_{ij}, i \neq j \mid \forall i, j \in \mathcal{N}$ control **the inter-target distance between T_{d_i} and T_{d_j}**

[1] J. Vilca, L. Adouane and M. Youcef, Stable and Flexible Multi-Vehicle Navigation Based on Dynamic Inter-Target Distance Matrix, IEEE Transactions on Intelligent Transportation Systems, vol 20, pp. 1416- 1431, 2019.

Inter-target distance matrix formalization

Safe inter-target gain:

The **inter-target distance** can be written as: $$d_T^2 = e_{f_{ij}}^T e_{f_{ij}} \qquad (7)$$

With $$e_{f_{ij}} = \left(f_i^{end} - f_i(t)\right) - \left(f_j^{end} - f_j(t)\right) = -e_{f_i} + e_{f_j} + e_{f_{ij}}^{end} \qquad (8)$$

Eq. (7) is derived to find the minimum inter-target distance: $$\frac{\partial(d_T^2)}{\partial t} = 2e_{f_{ij}}^T \dot{e}_{f_{ij}} = 0 \qquad (9)$$

We replace eq. (8) into eq.(9):

$$e_{f_{ij}}^T\left[(a_i - a_j + 2a_{ij})e_{f_i} - (a_{ij} - a_j)e_{f_{ij}}^{end}\right] = (a_{ij} - a_j)e_{f_{ij}}^T e_{f_{ij}} \qquad (10)$$

We use the minimum inter-target distance to express the inequality relation between eq. (10) and eq. (7):

$$e_{f_{ij}}^T\left[\frac{(a_i - a_j + 2\boldsymbol{a_{ij}})}{(\boldsymbol{a_{ij}} - a_j)} e_{f_i} - e_{f_{ij}}^{end}\right] \geq e_{f_{ij_{min}}}^T e_{f_{ij_{min}}} \qquad (11)$$

Further details can be found in [1].

$$A = \begin{bmatrix} a_1 & \boldsymbol{a_{12}} & \cdots & \boldsymbol{a_{1N}} \\ -\boldsymbol{a_{12}} & a_2 & \cdots & \boldsymbol{a_{2N}} \\ \vdots & \vdots & \ddots & \vdots \\ -\boldsymbol{a_{1N}} & -\boldsymbol{a_{2N}} & \cdots & a_N \end{bmatrix}$$

a_{ij}, $i \neq j \mid \forall i,j \in \mathcal{N}$ control **the inter-target distance between T_{d_i} and T_{d_j}**

[1] J. Vilca, L. Adouane and M. Youcef, Stable and Flexible Multi-Vehicle Navigation Based on Dynamic Inter-Target Distance Matrix, IEEE Transactions on Intelligent Transportation Systems, vol 20, pp. 1416- 1431, 2019.

Constrained optimal reconfiguration matrix

Constrained optimal reconfiguration matrix

Constrains aware convergence rate gains:

- Respect the environment constrains,
- Ensure the safety requirement.

$$A = \begin{bmatrix} \boldsymbol{a_1} & a_{12} & \cdots & a_{1N} \\ -a_{12} & \boldsymbol{a_2} & \cdots & a_{2N} \\ \vdots & \vdots & \ddots & \vdots \\ -a_{1N} & -a_{2N} & \cdots & \boldsymbol{a_N} \end{bmatrix}$$

$a_i \mid \forall i \in \mathcal{N}$ control **the convergence rate of the error**

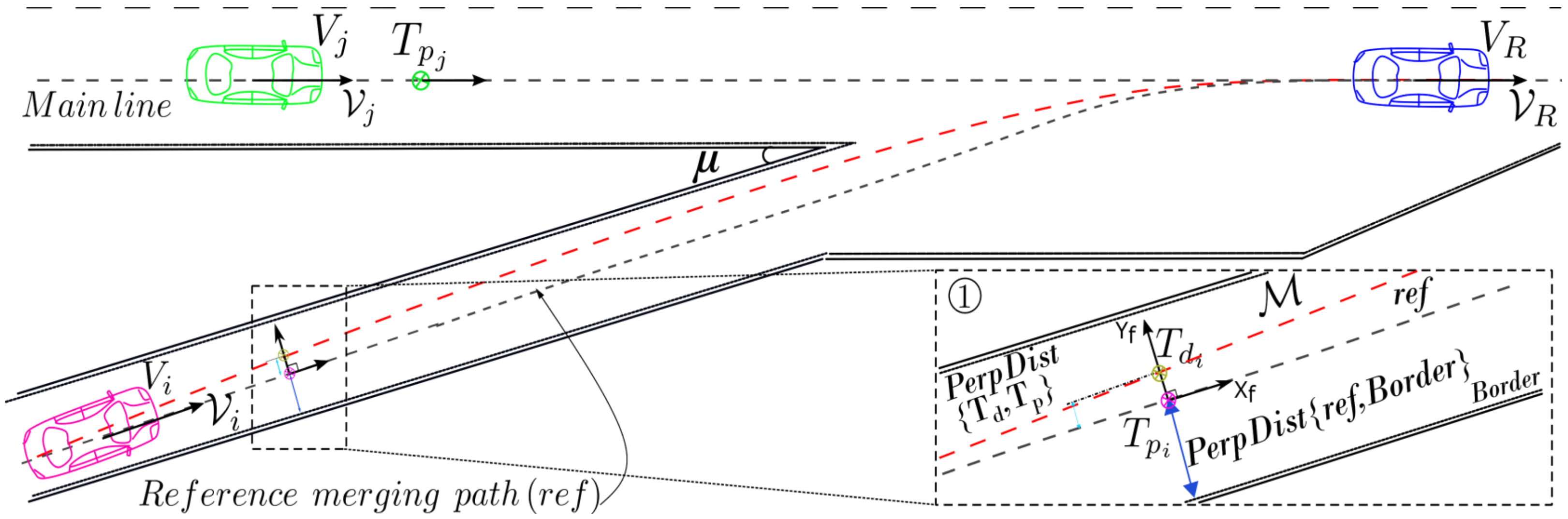

Fig 6. The projection of the dynamic target T_d w.r.t. the reference trajectory and the computation of the different distances allowing the optimization of the cost function in eq. (12)

The cost function used in the optimization of the convergence rate:

$$J_{\substack{a_i \\ \forall i \in \mathcal{N}}} = \sum_{k=0}^{T} \left[w_i \left[\frac{PerpDist\{T_{d_i}(t), T_{p_i}(t)\}}{PerpDist\{T_{p_i}(t), Border\}} \right]^2 + w_j \left[\frac{PerpDist\{T_{d_j}(t), T_{p_j}(t)\}}{PerpDist\{T_{p_j}(t), Border\}} \right]^2 \right] \qquad (12)$$

$\boldsymbol{w_{i,j}}$ are the optimization weights,

$\boldsymbol{PerpDist\{T_{d_{i,j}}(t), T_{p_{i,j}}(t)\}}$ perpendicular distance between $T_{d_{i,j}}$ and the projected target $T_{p_{i,j}}$ $\longmapsto$ needs to be minimized

$\boldsymbol{PerpDist\{T_{p_{i,j}}(t), Border\}}$ perpendicular distance between $T_{p_{i,j}}$ and the border of the road $\longmapsto$ used for normalization

Constrained optimal reconfiguration matrix

Optimization approach:

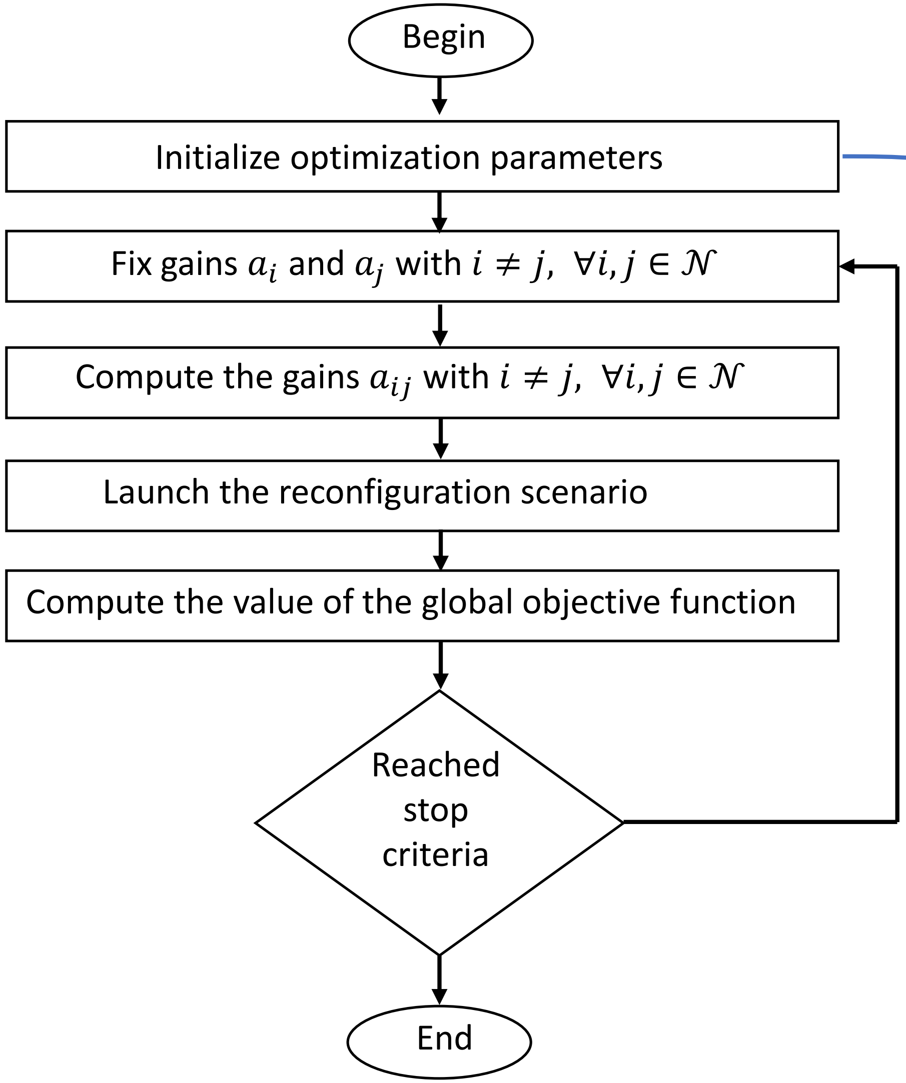

Fig 7. The proposed optimization algorithm flowchart

Algorithm 1: Optimization Algorithm

Input : $GlobalInput$ Scenario data
$[a_{i_{min}}, a_{i_{max}}]^T$ boundaries of the gain a_i
$[a_{j_{min}}, a_{j_{max}}]^T$ boundaries of the gain a_j
$[a_{i_0}, a_{j_0}]^T$ start point of the optimization
$ObjectiveFunction$ the objective function in eq. (10)

Output : $[a_i^*, a_j^*]^T$ optimal values of the gains a_i and a_j

$MergingData \leftarrow [PerpDist\{T_{d_i}, T_{p_i}\}, PerpDist\{T_{d_j}, T_{p_j}\}, PerpDist\{T_{p_i}, Border\}, PerpDist\{T_{p_j}, Border\}]^T$
while $(StopCriteria \neq True)$ **do**
  $[a_i, a_j]^T \leftarrow Fixe([a_{i_0}, a_{j_0}]^T, [a_{imin}, a_{imax}]^T, [a_{jmin}, a_{jmax}]^T)$
  $MergingData \leftarrow MergingScenario(GlobalInput, a_i, a_j)$
  $T \leftarrow length(MergingData)$
  forall $t \in [0, T]$ **do**
    $Cost(t) \leftarrow ObjectiveFunction(MergingData(t))$
  $GlobalCost \leftarrow Sum(Cost)$

However

The dynamic of the target T_d

≠

the dynamic of the projected target T_p

Safe and feasible on-ramp merging maneuver

Safe and smooth projected target $\bar{T}_p$ dynamic:

We draw advantage from the optimal inter-target distance matrix in terms of safety, to compute the *necessary mean velocity* imposed to the projected target $\bar{T}_p$.

Mean velocity ⟶ $CAVs$ V_i and V_j enter *the conflicting zone* at the same moment as if they have followed T_d

$$EucDist\left\{\bar{T}_{p_j}(t_{end}), \bar{T}_{p_i}(t_{end})\right\} = EucDist\left\{T_{d_j}(t_{end}), T_{d_i}(t_{end})\right\} \qquad (12)$$

Definition of the conflicting zone:

Conflicting zone:
It defines the intersection between the surroundings circles of both the CAV V_i and CAV V_j

- $P_{merging}$ position of V_j where $Conflict\ zone \neq \emptyset$

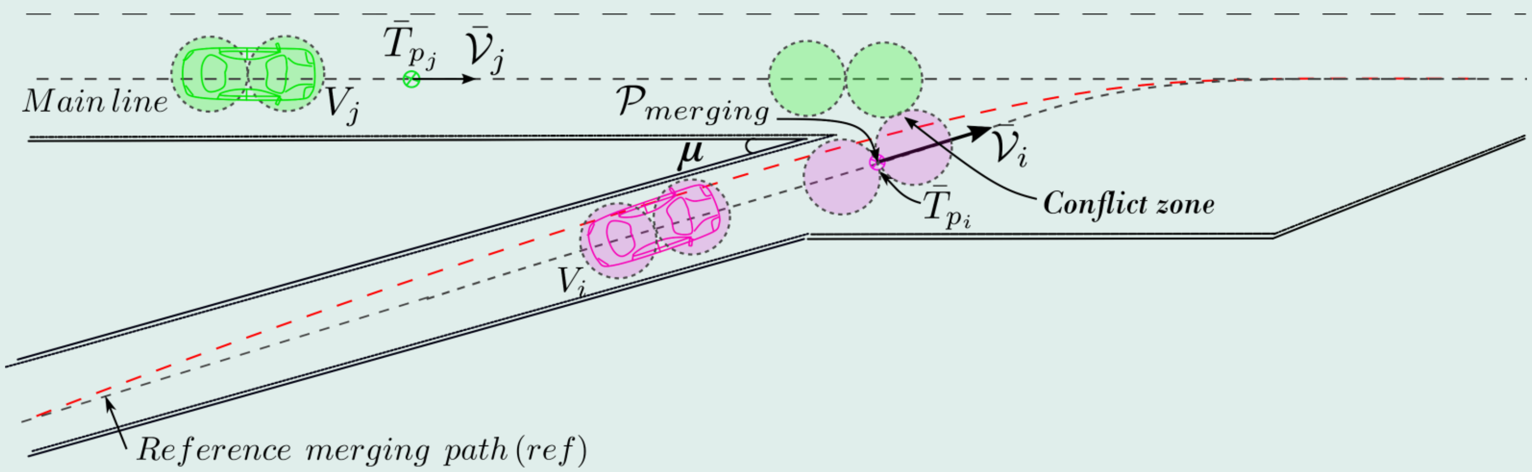

Fig 8. Definition of the conflicting zone

Safe and feasible dynamic:

Computation of the safe mean velocity imposed to T_p:

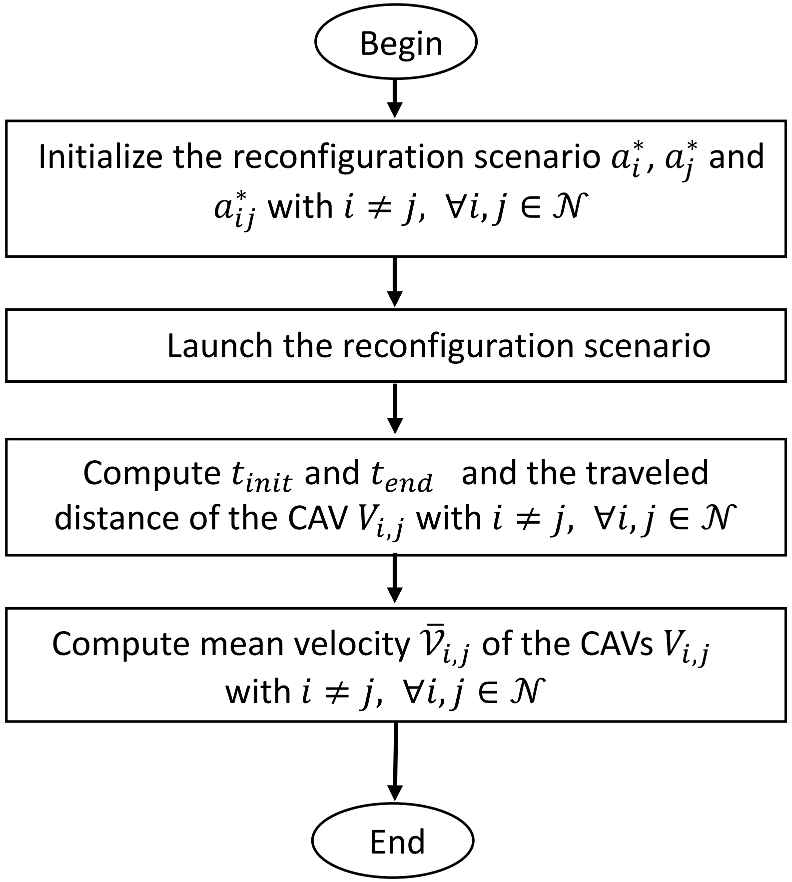

Fig 9. The flowchart of the computation of the mean velocity $\bar{\mathcal{V}}$ imposed to T_p

Algorithm 2: Projections and computation of the imposed dynamic

Input : $GlobalInput$ Scenario data
a_i^*, a_j^*, a_{ij}^* optimal gains of the reconfiguration matrix (cf. Algorithm 1)
Output : $\bar{\mathcal{V}}_{i,j}$ the mean velocity of the vehicles V_i and V_j

$k \leftarrow 1$
$\mathcal{F}(k) \leftarrow \mathcal{F}^{init}$
$\varepsilon(k) \leftarrow \mathcal{F}^{end} - \mathcal{F}(k)$
$Buffer_R \leftarrow ReferenceTrajectory(V_R)$
$Buffer_{i,j} \leftarrow ReferenceTrajectory(V_i, V_j)$
while $(\varepsilon(k) \neq 0)$ **do**
  $k \leftarrow k+1$
  $\mathcal{F}(k) \leftarrow DynamicReconfiguration(\mathcal{F}^{end}, \mathcal{F}(k-1))$
  $\varepsilon(k) \leftarrow \mathcal{F}^{end} - \mathcal{F}(k)$
  $T_{d_{i,j}}(k) \leftarrow Transform(Buffer_R, \mathcal{F}(k), X_{V_R})$
  $T_{p_{i,j}}(k) \leftarrow Projection(Buffer_{i,j}, T_{d_{i,j}})$
  $X_{V_{i,j}}(k) \leftarrow Control(X_{V_{i,j}}(k-1), T_{p_{i,j}}(k))$
$\bar{\mathcal{V}}_{i,j} = \frac{CurviDist\{V_{i,j}(1,k)\}}{t_{end} - t_{init}}$

Smooth velocity profile:

A **sigmoidal function** is used to generate the velocity profile of T_p.

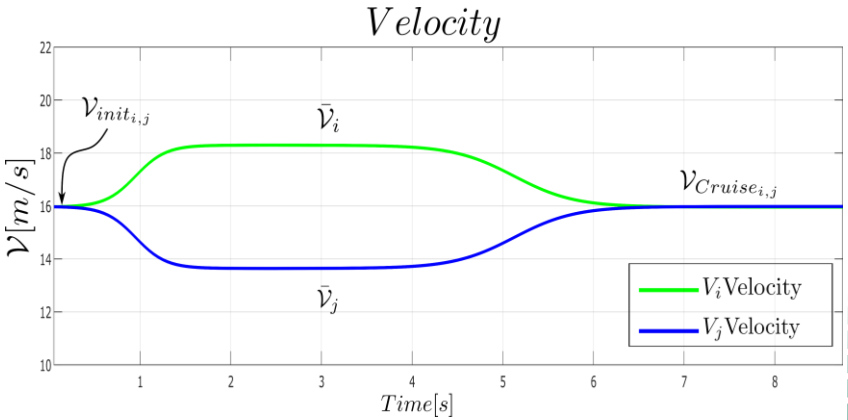

Fig 10. The sigmoidal function used to generation of the velocity profiles

The sigmoidal function takes into account:

- The initial velocity $\mathcal{V}_{init}$,
- The mean velocity $\bar{\mathcal{V}}_{init}$,
- The cruising velocity $\mathcal{V}_{cruise}$,
- The slope is saturated to respect acceleration and deceleration limits.

Simulation results

Simulation scenario:

Context:

Three vehicles participate into the on-ramp merging on highway maneuver:

- **CAV V_1** considered as the **reference CAV**,
- **CAV V_2** already in the **main line** and behind V_1 ($40m$ distance separate them),
- **V_3 the merging CAV**, behind both V_1 and V_3

The goal:

Perform the merging of CAV V_3 between CAV V_1 and V_2, while ensuring the respect of the minimum safety distance $\underline{D}_T$ and the smoothness of the merging maneuver.

Tab I. The values of the inputs of the CORM algorithm

Inputs	Values
Initial formation coordinates $[m]$	$\begin{pmatrix} 0 & -40 & -50 \\ 0 & 0 & 9.2 \end{pmatrix}$
Final formation coordinates $[m]$	$\begin{pmatrix} 0 & -80 & -40 \\ 0 & 0 & 0 \end{pmatrix}$
$V_{1,2,3}[m/s]$	$[19.4, 19.4, 19.4]$
$[a_{2min}, a_{2max}]^T$	$[-0.4, 0.1]$
$[a_{3min}, a_{3max}]^T$	$[-0.4, -0.05]$
$[a_{2_0}, a_{3_0}]^T$	$[-0.25, -0.25]$
$[w_2, w_3]^T$	$[1, 4]$
$[a_2^*, a_3^*]^T$	$[-0.1228, -0.365]$
$\underline{D}_T[m]$	12

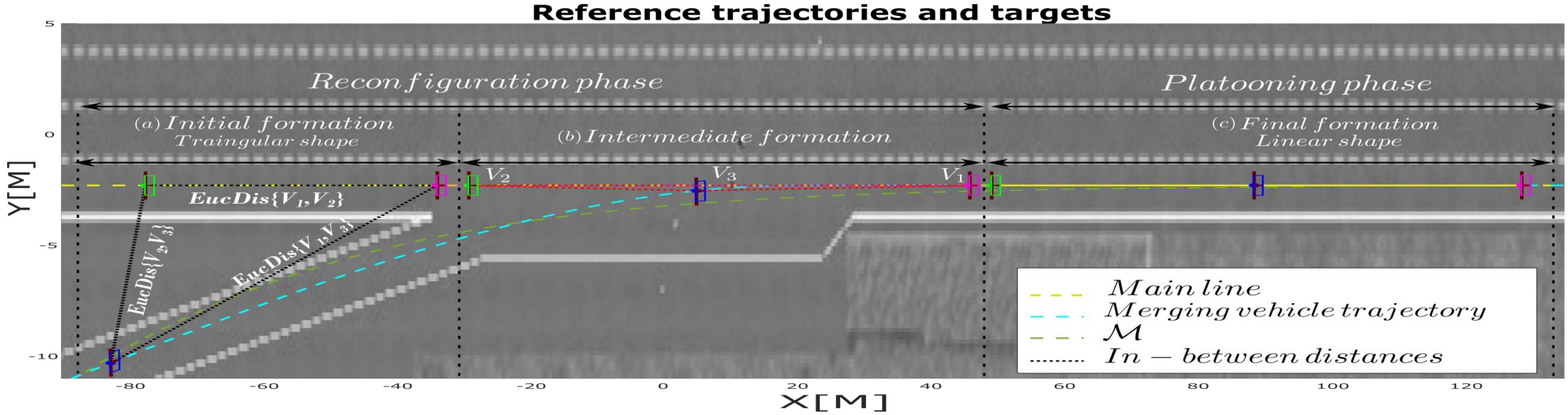

Fig 10. Evolution of the virtual structure shape while the on-ramp is being performed

Simulation video: on-ramp merging using the CORM algorithm

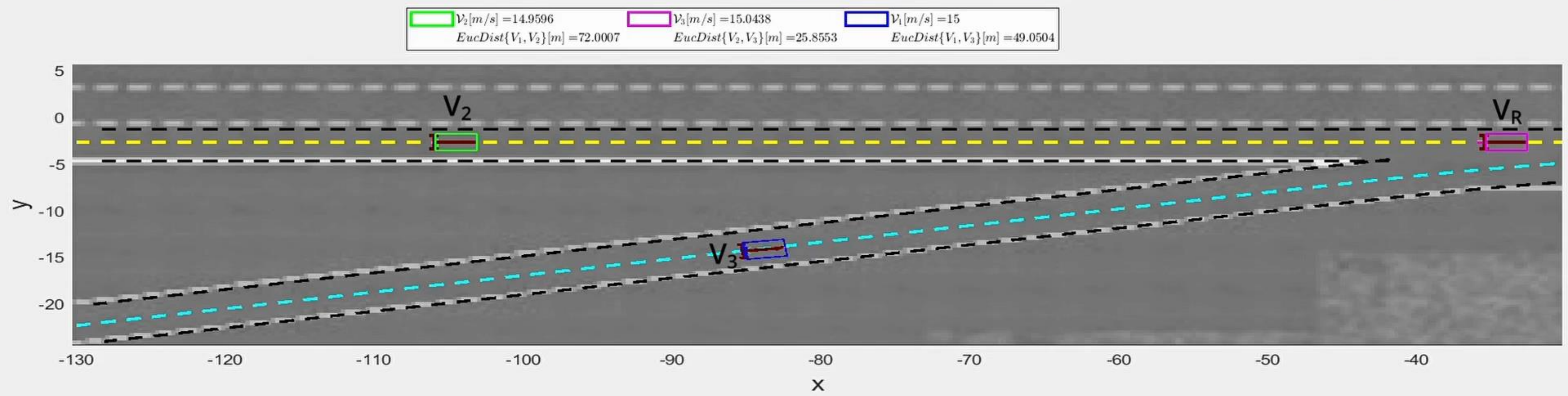

Simulation results

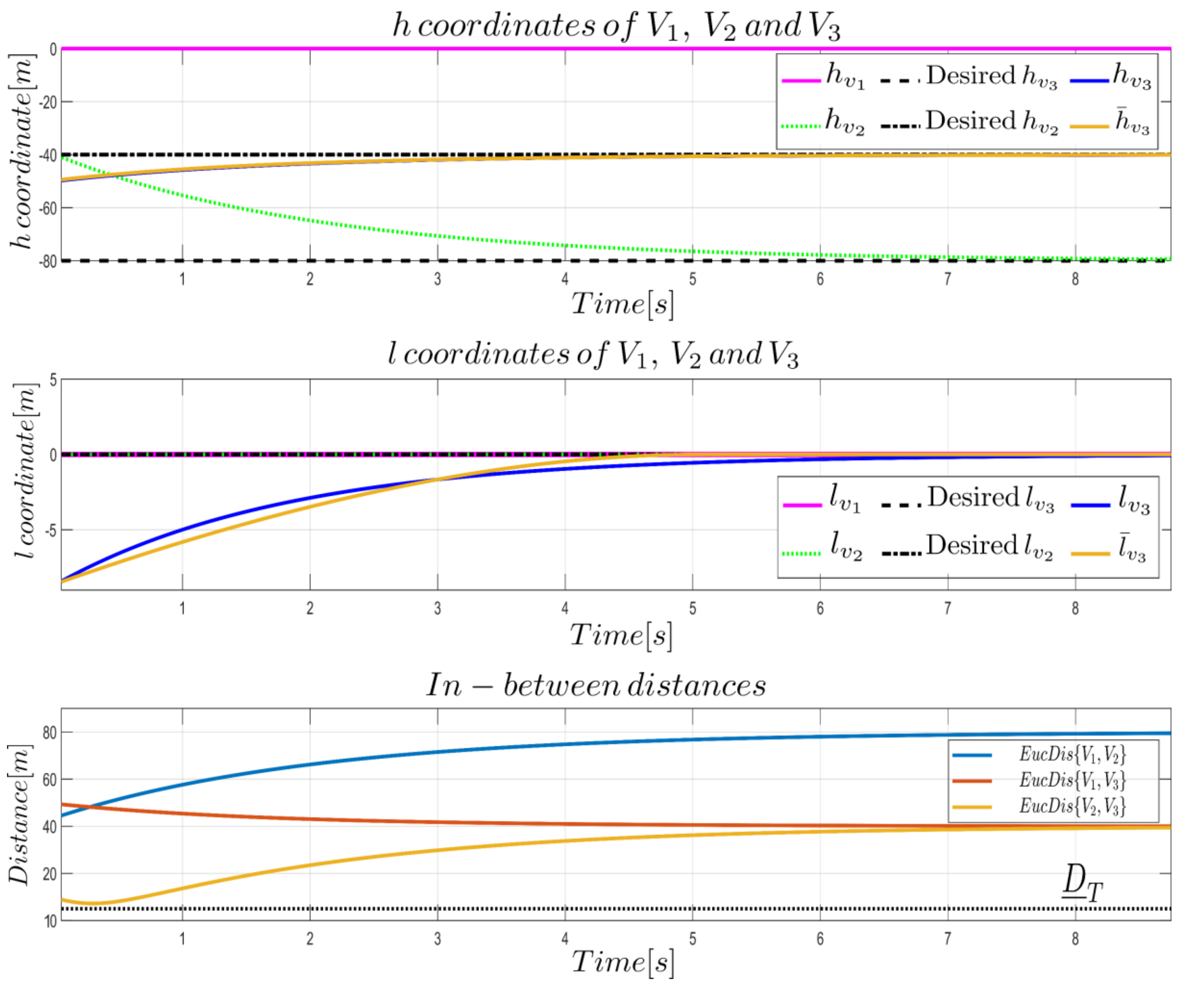

Fig 11. Formation coordinates and in-between distances evolution

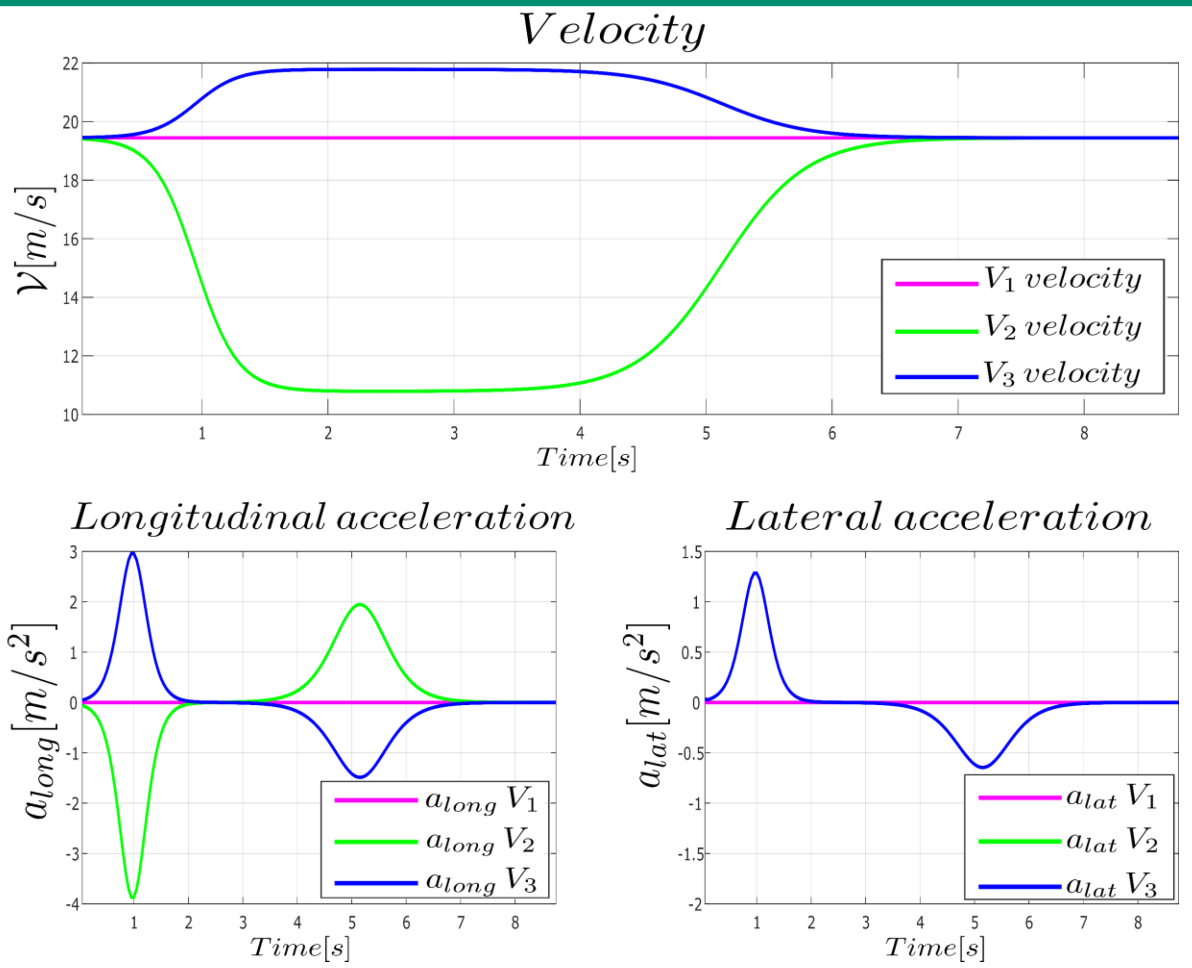

Fig 12. Velocity and acceleration profiles

In summary:

- The virtual structure shape convergences from its initial toward its desired final one as shown in the plots of the shape coordinates.
- The in-between distances are safe, as they are always greater than the minimum safety distance $\underline{D}_T$.
- The merging maneuver is smoothly performed according the velocity, longitudinal and lateral acceleration plots.

Influence of the projection phase on the CORM algorithm efficiency:

Context:

In order to conclude on the influence of the projection phase w.r.t. the CORM Efficiency, intensive tests were conducted with the following parameters:

- $10° \leq \mu \leq 30°$ with a $\Delta\mu = 10°$
- $\forall\mu$, the cruising velocity $\mathcal{V}_R$,$5\text{ m/s} \leq \mathcal{V}_R \leq 15m/s$ with $\Delta\mathcal{V} = 5m/s$

Goal:

The goal of the simulations is to conclude on the respect of the safety requirement along with the smoothness of the performed Maneuver.

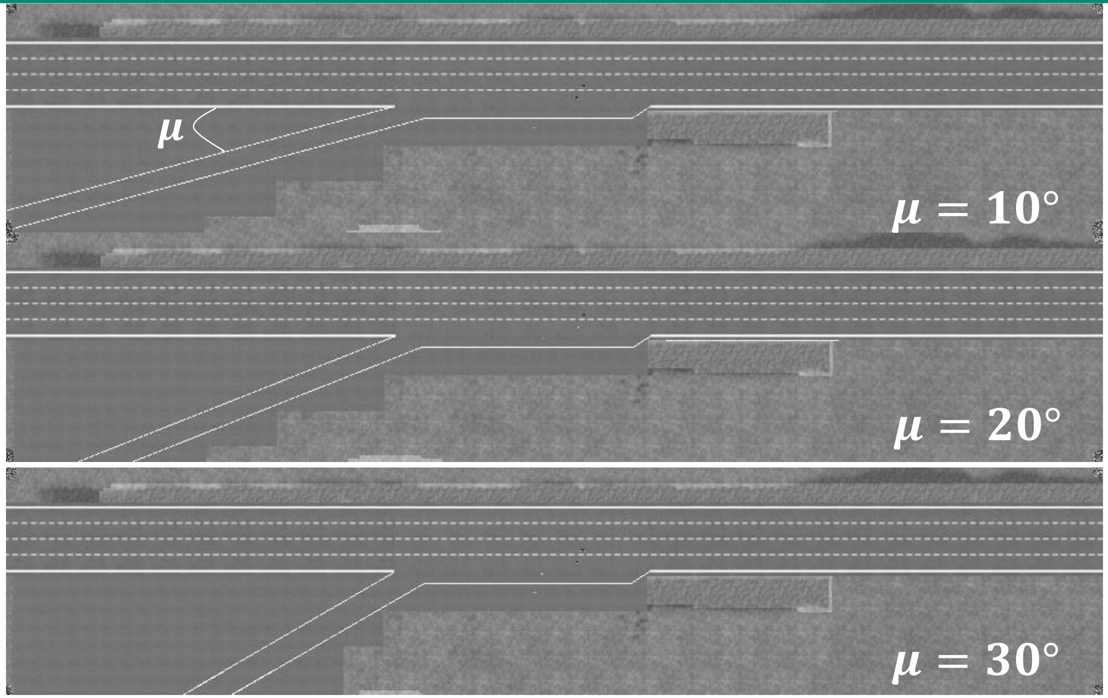

Fig 13. Top-view of the on-ramp merging scenario

Tab II. The summary results of the conducted simulation for a variable incidence angle μ and CAVs velocity $\mathcal{V}$

μ[deg]	10			20			30		
$\mathcal{V}_R[m/s]$	5	10	15	5	10	15	5	10	15
$[\mathcal{V}_{2min}, \mathcal{V}_{2max}][m/s]$	[4.36, 5]	[8.73,10]	[13.45, 15]	[4.21, 5]	[8.49,10]	[13.26, 15]	[4.13, 5]	[8.35,10]	[13.06,15]
$[\mathcal{V}_{3min}, \mathcal{V}_{3max}][m/s]$	[5,5.59]	[10,11.125]	[15,16.80]	[5,5.824]	[10,11.6316]	[15,17.43]	[5,6.10]	[10,12.10]	[15,18.14]
$[a_{2min}, a_{2max}]_{long}[m/s^2]$	[-0.29, 0.15]	[-0.60, 0.29]	[-0.70, 0.35]]	[-0.35, 0.18]	[-0.68, 0.34]	[-0.78, 0.53]	[-0.38,0.19]	[0.70,0.37]	[-0.87,0.44]
$[a_{2min}, a_{2max}]_{lat}[m/s^2]$	[0,0]	[0,0]	[0,0]	[0,0]	[0,0]	[0,0]	[0,0]	[0,0]	[0,0]
$[a_{3min}, a_{3max}]_{long}[m/s^2]$	[-0.76,1.52]	[-1.66, 2.02]	[-1.14,2.27]	[-0.570,1.07]	[-1.66, 2.02]	[-1.54,2.92]	[-0.65,1.39]	[-1.31,2.55]	[-2.00,2.75]
$[a_{3min}, a_{3max}]_{lat}[m/s^2]$	[-0.29,0.74]	[-0.39,0.80]	[-0,74,1.38]	[-0.84,0.75]	[-1.02,0.96]	[-1.60,1.59]	[-1.56,1.55]	[-2.23,1.94]	[-3.63,2.53]
$D[m]$	21.66	21.80	23.30	24.75	24.01	23.30	28.70	27.30	25.725
$Error_{max}[m]$	0.52	0.73	0.78	0.85	0.88	0.92	1.10	1.13	1.14

Conclusion and perspectives

Conclusion and perspectives

- Safe and smooth on-ramp merging approach for Cooperative and Automated Vehicles (CAVs).
- A two steps Constrained Optimal Reconfiguration Matrix (CORM):
    1. An Optimization algorithm that ensures the performance of the merging maneuver using safe dynamic targets within the virtual structure, while taking into account the environment constraints,
    2. Safe and feasible projection based approach adapter for the on-ramp merging.
- Several simulations were conducted in order to test the performance of the CORM algorithm.

Future work:

- Compare the performance of the CORM algorithm to other on-ramp merging approaches.
- Implementation of the proposed method into a real vehicle.

Thank you !
Questions ?

Contact at: lyes.saidi@hds.utc.fr